JOURNAL OF CATALYSIS 121, 1–6 (1990)

# A Comment on the Analysis of CO Hydrogenation Using the BOC-MP Approach

ALEXIS T. BELL* AND EVGENY SHUSTOROVICH†

*Center for Advanced Materials, Lawrence Berkeley Laboratory, and Department of Chemical Engineering, University of California, Berkeley, California 94720; and †Corporate Research Laboratories, Eastman Kodak Company, Rochester, New York 14650

Received March 1, 1989; revised August 16, 1989

In a recent paper (*1*), an analysis was presented of CO hydrogenation pathways on the (111) surface of Ni, Pd, and Pt, using the bond-order conservation Morse-potential (BOC-MP) method (*2*). Included were calculations of the heats of adsorption of all reactants, intermediates, and products, and activation energies for the elementary processes involved in the formation of methane and methanol. Since the publication of this paper, the BOC-MP method of calculating the activation energy for the dissociation of diatomic species as well as the heat of chemisorption of molecular fragments (radicals) has been significantly improved (*3, 4*). This has made it possible to treat chemisorption, dissociation, and recombination of diatomic and polyatomic species in a straightforward manner, without recourse to the rather intuitive and not well defined procedure of bond-energy partitioning used earlier (*1*) for polyatomic adsorbates. The purpose of this communication is to comment on the effects of these new developments.

The improvements in calculating the activation energy for the dissociation of a diatomic molecule $AB$ can be understood with the aid of Fig. 1. The conventional one-dimensional Lennard–Jones (LJ) potential diagram defines the transition state for dissociation as the intersection point of the molecular $AB$ and atomic $A + B$ curves. Accordingly, the energy of the transition state may be calculated from the atomic components, from which it can be inferred that the $A$–$B$ bond order in the transition state is zero. Then, within the BOC-MP framework, the activation energy for $AB$ dissociation from the gas phase, $\Delta E^{*,\mathrm{LJ}}_{AB,\mathrm{g}}$, is given by (*2*)

$$\Delta E^{*,\mathrm{LJ}}_{AB,\mathrm{g}} = D_{AB} - (Q_A + Q_B) + Q_A Q_B/(Q_A + Q_B), \quad (1)$$

where $D_{AB}$ is the gas-phase dissociation bond energy, and $Q_A$ and $Q_B$ are the heats of adsorption for atoms $A$ and $B$, respectively. The difficulty with the LJ description of $AB$ dissociation is that it relies on a one-dimensional representation of the system energy as a function of the reaction coordinate, $R$, which is usually taken as the surface–$AB$ distance. In reality, both the $AB$ and the $A + B$ energy profiles are multidimensional hypersurfaces the coordinates for which include not only the metal–$A$ and metal–$B$ distances but also the $A$–$B$ distance. It is, therefore, realistic to expect that in the transition state, the $A$–$B$ bond order is greater than zero. The assumption of a finite $A$–$B$ bond order in the transition state leads to a reduction in the calculated activation energy for dissociation of the $A$–$B$ bond (*2, 3*). Since the dissociation of $AB$ should occur somewhere between the $AB$ chemisorption state and the LJ dissociation point (see Fig. 1), the simplest interpolation puts the dissociation barrier in the middle of this energy interval, namely (*3*),

$$\Delta E^{*}_{AB,\mathrm{g}} = 0.5\,(\Delta E^{*,\mathrm{LJ}}_{AB,\mathrm{g}} - Q_{AB}), \quad (2)$$



0021-9517/90 $3.00

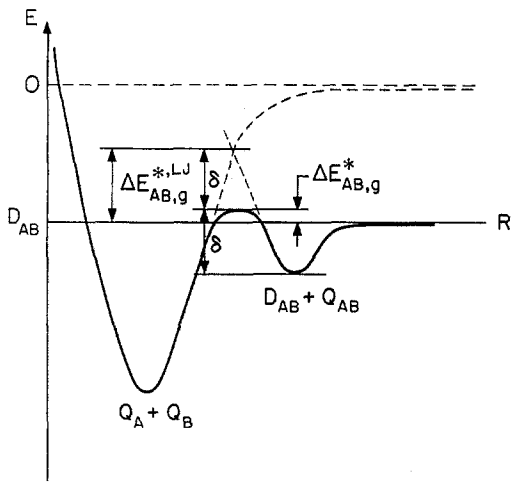


FIG. 1. The potential energy diagram for *AB* dissociation.

where $Q_{AB}$ is the heat of adsorption for the molecule *AB*. By so doing we effectively calculate the multidimensional activation barrier. Figure 1 shows that the activation barrier $\Delta E^*_{AB,s}$ for dissociation from the chemisorbed state is larger than the activation barrier $\Delta E^*_{AB,g}$ for dissociation from the gas phase by the amount of $Q_{AB}$,

$$\Delta E^*_{AB,s} = \Delta E^*_{AB,g} + Q_{AB}. \qquad (3)$$

Equation (2) has been found (*3*) to provide good agreement with experimentally observed activation energies for dissociative adsorption of $H_2$, $N_2$, and CO on various transition metal surfaces. In particular, as illustrated in Table 1, only Eq. (2) is able to project the negative values of $\Delta E^*_{CO,g}$ for the thermal dissociation of CO that have been reported for Ni(100) (*6*), Fe(111) (*7a*), Mo(100) (*7b*), and W(110) (*7c*).

The improvement in calculating the heat of chemisorption of molecular radicals *AB* stems from the realization that radicals such as CH, $CH_2$, OH, and NH chemisorb similarly to atoms. By this it is meant that such radicals are adsorbed strongly and typically prefer hollow sites of the highest coordination, unlike closed-shell molecules such as CO, $H_2O$, and $NH_3$ which are adsorbed more weakly and exhibit a weak sensitivity to the metal coordination number. Mathematically, the sole difference between the "strong" and "weak" extremes is the choice of the Morse constant *Q* describing the effective $M_n$–*A* interaction

TABLE 1

Activation Energy for CO Dissociation[a]

| Surface | $Q_A$ | $Q_B$ | $Q_{AB}$ | $\Delta E^*_{AB,g}$ | | Exp.[b] |
|---|---|---|---|---|---|---|
| | | | | Eq. (1) | Eq. (2) | |
| Ni(111) | 171 | 115 | 27 | 40 | 6.5 | – |
| Ni(100) | 171 | 130[c] | 30 | 30 | ~0 | −3[d]; −7[e] |
| W(110) | 200 | 125 | 21[f] | 9 | −6 | −15[f] |
| Fe(111) | (200)[g] | (125)[g] | 32[h] | 9 | −6 | −12[h] |
| Mo(100) | (200)[g] | (125)[g] | 16[i] | 9 | −6 | −2[i] |

[a] If not otherwise stated, experimental values of $Q_A$, $Q_B$, and $Q_{AB}$ are taken from Ref. (*2*). All energies in kcal/mol.

[b] From the experimental estimates of $\Delta E^*_{CO,g}$ via Eq. (3).

[c] Ref. (*5*).

[d] Ref. (*6b*).

[e] Ref. (*6a*).

[f] Ref. (*7c*).

[g] Assumed to be the same as for W(110) [see Ref. (*3*)].

[h] Ref. (*7a*).

[i] Ref. (*7b*).

for $M_n$–$AB$ chemisorption, namely, $Q_A$ and $Q_{oA}$, respectively, which interrelate as $Q_A = Q_{oA}(2 - 1/n)$ (*2*). In our previous work (*1*, *2*), we have assumed $Q = Q_{oA}$, which leads to

$$Q_{AB} \simeq \frac{Q_{oA}^2}{(Q_{oA}/n) + D_{AB}} \quad \text{for } D_{AB} > (n-1)/n\, Q_{oA} \quad (4)$$

This equation has proved to be highly accurate for calculating $Q_{AB}$ for CO, $H_2O$, and $NH_3$ (*2*), where, typically, the $AB$ molecules are coordinated in the on-top site ($n = 1$) and the values of $Q_{AB}$ are smaller than those of $Q_A$ by a factor of 5–10.

On the other hand, if we assume $Q = Q_A$, the same BOC-MP variational procedure (*3*) gives

$$Q_{AB} \simeq \frac{Q_A^2}{Q_A + D_{AB}}. \quad (5)$$

As discussed in Ref. (*3*), Eq. (5) is much more accurate than Eq. (4) for calculating $Q_{AB}$ for CH, $CH_2$, OH, $OCH_3$, and NH.

For monovalent radicals of tetra- and trivalent atoms such as C and N in $CH_3$, HCO, or $NH_2$, which are intermediate in character between closed shell molecules and polyvalent radicals, the value of $Q_{AB}$ is taken as the arithmetic average of Eqs. (4) and (5), namely (*3*),

$$Q_{AB} = 0.5\left[\frac{Q_{oA}^2}{(Q_{oA}/n) + D_{AB}} + \frac{Q_A^2}{Q_A + D_{AB}}\right]. \quad (6)$$

With these improvements in calculating the molecular heats of chemisorption, the dissociation barriers $\Delta E_{AB}^*$ for both di- and polyatomic adsorbates can be uniformly calculated by using Eqs. (1)–(3), where $D_{AB}$ is the difference between the total gas-phase bond energies of $AB$ and $A + B$. The barriers for recombination of $A_s$ and $B_s$, $\Delta E_{A-B}^*$, can also be determined uniformly from the relevant thermodynamic relationships between $\Delta E_{A-B}^*$, $\Delta E_{AB}^*$, and the enthalpy difference $\Delta H = \Delta H_{AB} - \Delta H_{A+B}$.

Table 2 lists the new values of $Q_{AB}$ for all species thought to be involved in the hydrogenation of CO. The new values of $\Delta E_{AB}^*$ and $\Delta E_{A-B}^*$ for each elementary step thought to contribute to the formation of $CH_4$ and $CH_3OH$ are listed in Tables 3 and 4.

A major objective of our work is to understand why CO hydrogenation on Ni leads only to $CH_4$ but on Pd and Pt can result in the formation of both $CH_4$ and $CH_3OH$. As seen from Table 2, the formations of $CH_4 + H_2O$ and $CH_3OH$ from CO and $H_2$ are both exothermic processes, the former being more exothermic than the latter by 27 kcal/mol. Since the methanation of CO is thermodynamically more favorable, the only chance for producing methanol selectively is to have a catalyst on which the hydrogenation of $H_xCO_s$ ($x$ = 0–3) species is preferred kinetically over $H_xC$–O bond cleavage, that is on catalysts for which the hydrogenation barriers are distinctly smaller than the barriers for $H_xC$–O bond cleavage. An appreciation of how metal composition influences both the activation barriers and the enthalpies of the steps involved in the formation of methane and methanol can be obtained from an examination of the results presented in Tables 2–4.

We begin by considering the pathways for the formation of methane. It is evident from Table 3 that on Ni the activation energy for CO hydrogenation to form $HCO_s$ is 10 kcal/mol less than that for the dissociation of $CO_s$ to produce $C_s$ and $O_s$. However, because the activation barrier for formyl decomposition back to $H_s$ and $CO_s$ is zero and all other processes involving formyl species have large positive activation energies, formyl species would not be expected to accumulate on a Ni(111) surface to any significant extent. By contrast, $CO_s$ dissociation, which has a moderate activation barrier of 33 kcal/mol, is a nearly thermoneutral process and consequently we project the accumulation of significant

TABLE 2

Zero-Coverage Heats of Chemisorption ($Q$) and Total Bond Energies in the Gas Phase ($D$) and in Chemisorbed States ($D + Q$) on Ni(111), Pd(111), and Pt(111)[a]

| Species | $D$[b] | Ni(111) | | Pd(111) | | Pt(111) | |
|---|---|---|---|---|---|---|---|
| | | $Q$ | $D+Q$ | $Q$ | $D+Q$ | $Q$ | $D+Q$ |
| C | — | 171 | 171 | 160 | 160 | 150 | 150 |
| CH | 81 | 116 | 197 | 106 | 187 | 97 | 178 |
| $CH_2$ | 183 | 83 | 266 | 75 | 258 | 68 | 251 |
| $CH_3$ | 293 | 48 | 341 | 42 | 335 | 38 | 331 |
| $CH_4$ | 398 | 6[c] | 404 | 6[c] | 404 | 6[c] | 404 |
| H | — | 63 | 63 | 62 | 62 | 61 | 61 |
| O | — | 115 | 115 | 87 | 87 | 85 | 85 |
| OH | 102 | 61 | 163 | 40 | 142 | 39 | 141 |
| $OH_2$ | 220 | 17 | 237 | 10 | 230 | 10 | 230 |
| $OCH_3$ | 383 | 65 | 448 | 43 | 426 | 41 | 424 |
| $CH_3OH$ | 487 | 18 | 505 | 11 | 498 | 11 | 498 |
| CO | 257 | 27[d] | 284 | 34[d] | 291 | 32[d] | 289 |
| HCO | 274 | 50 | 324 | 44 | 318 | 40 | 314 |
| $H_2CO$ | 361 | 19 | 380 | 12 | 373 | 11 | 372 |

[a] See text for the relevant formulas and explanations. All energies in kcal/mol.

[b] Ref. (*8*).

[c] Taken as the experimental value of $Q_{CH_4} = 6$ kcal/mol on Rh (*9*).

[d] Experimental values (*2*).

amounts of $C_s$, in good agreement with experimental observation (*10a*).

A further point brought out by Table 3 is that the activation barrier for the hydrogenation of $C_s$ to $CH_s$ is 9 kcal/mol higher than that for the dissociation of $CO_s$ to $C_s$ and $O_s$. It is also seen that the activation barriers for the subsequent hydrogenation of $CH_s$ to $CH_{4,g}$ are all significantly smaller than that for $CH_s$ formation. Thus, on the basis of energetic considerations we project that for methanation on Ni, the rate-determining step is hydrogenation of $C_s$ to form $CH_s$. Consistent with this, Goodman and Campbell (*8a*) have shown that potassium promotion of Ni(100) results in a reduction of the activation barrier for CO dissociation but not of the apparent activation energy for CO hydrogenation to $CH_4$, suggesting that CO dissociation is not the rate-limiting step. Our projections are also in agreement with the observations of Yates *et al.* (*11*), who have found that on Ni(111) the rate of $CH_4$ formation via hydrogenation of $CH_{3,s}$ is six orders of magnitude faster than the rate of $CH_4$ formation obtained via CO hydrogenation, suggesting that the rate-limiting step occurs before the hydrogenation of $CH_{3,s}$ to $CH_4$.

Our calculations make it easy to understand why methanol cannot be formed on Ni. Table 4 shows that the C–O bond cleavage as $HCO_s \rightarrow C_s + OH_s$ is preferred over hydrogenation $HCO_s + H_s \rightarrow H_2CO_s$ (the barriers are 18 and 33 kcal/mol, respectively) and that the reaction $CH_3O_s \rightarrow CH_{3,s} + O_s$ is preferred over the reaction $CH_3O_s + H_s \rightarrow CH_3OH_s$ (the barriers are 13 and 19 kcal/mol, respectively). Moreover, if $CH_3OH_s$ could somehow be formed, the desorption of methanol would not occur since the barrier for desorption is larger (by 5 kcal/mol) than that for dissociation back to $CH_3O_s$ and $H_s$, consistent with the LITD

TABLE 3

Zero-Coverage Activation Barriers for Forward ($\Delta E_f^*$) and Reverse ($\Delta E_r^*$) Elementary Reactions for Methanation on Ni(111) and Pd(111)[a]

| Reaction | $\Delta E_f^*$ | | $\Delta E_r^*$ | |
|---|---|---|---|---|
| | Ni | Pd | Ni | Pd |
| $CO_s \rightleftarrows C_s + O_s$ | 33 | 50 | 35 | 6 |
| $H_s + C_s \rightleftarrows CH_s$ | 42 | 40 | 5 | 5 |
| $H_s + CH_s \rightleftarrows CH_{2,s}$ | 17 | 15 | 23 | 24 |
| $H_s + CH_{2,s} \rightleftarrows CH_{3,s}$ | 12 | 9 | 24 | 24 |
| $H_s + CH_{3,s} \rightleftarrows CH_{4,g}$ | 14 | 9 | 8 | 10 |
| $H_s + CH_{3,s} \rightleftarrows CH_{4,s}$ | 14 | 9 | 14 | 15 |
| $H_s + CO_s \rightleftarrows HCO_s$ | 23 | 35 | 0 | 0 |
| $HCO_s \rightleftarrows CH_s + O_s$ | 35 | 46 | 23 | 2 |
| $\rightleftarrows C_s + OH_s$ | 18 | 24 | 28 | 8 |
| $CO_s + H_s \rightleftarrows CH_s + O_s$ | 58 | 81 | 23 | 2 |
| $\rightleftarrows C_s + OH_s$ | 41 | 59 | 28 | 8 |

[a] See Table 2 for the values of $Q$ and $D + Q$ used in the calculations of $\Delta E^*$. All energies in kcal/mol.

measurements by Hall *et al.* (*12*). Thus, on Ni the activation barriers associated with the elementary steps for methanol formation are persistently less favorable than those leading to methane.

For Pd(111), the activation barrier for $CO_s$ dissociation is high (50 kcal/mol) and 15 kcal/mol greater than that for $CO_s$ hydrogenation to $HCO_s$. Moreover, in contrast to Ni(111), $CO_s$ dissociation is now found to be a highly endothermic process, and hence, a significant accumulation of carbon is not expected. Other important differences between Pd(111) and Ni(111) are also observed. The first is that the activation barrier for hydrogenation of $HCO_s$ to $H_2CO_s$ is lower by 8 kcal/mol than the barrier for $HCO_s$ dissociation to $CH_s$ + $O_s$. Again, in contrast to Ni(111), the hydrogenation $CH_3O_s + H_s \rightarrow CH_3OH_s$ is preferred over the process $CH_3O_s \rightarrow CH_{3,s} + O_s$, and $CH_3OH_s$ can be desorbed intact since the activation barrier for desorption is significantly smaller than that for dissociation (11 versus 22 kcal/mol, respectively). Based on these considerations, we project that on Pd(111) stepwise hydrogenation of $CO_s$ to $CH_3OH$ is a favorable process.

Because of the large endothermicity of $CO_s$ dissociation on Pd(111) and the very high activation barrier for this process, it is unlikely that C–O bond cleavage will occur by direct dissociation of $CO_s$. Tables 3 and 4 indicate that the more likely pathways for C–O bond cleavage are via the dissociation of $H_xCO_s$ ($x$ = 1, 3). Thus, compared to Ni(111), hydrogen-assisted dissociation of CO is predicted to be much more important on Pd(111), in agreement with experimental observation (*13, 14*).

Finally, we note that Battacharya *et al.* (*15*) have recently reported EELS observations of $CH_3O_s$ species upon annealing $CH_3OH$ adsorbed on Pd(110) to 200 K. Raising the annealing temperature to 300 K resulted in the appearance of new features in the EELS spectrum, which were attributed to $HCO_s$, and possibly $H_2CO_s$. These results support the projections of the BOC-MP method that $HCO_s$, $H_2CO_s$, and $CH_3O_s$ are intermediates in the synthesis of $CH_3OH$ from CO on Pd surfaces. Another piece of supporting evidence comes from an isotopic tracer study of $CH_3OH$ ($H_3{}^{12}C^{18}OH$ and $H_3{}^{13}C^{16}OH$) decomposition of

TABLE 4

Zero-Coverage Activation Barriers for Forward ($\Delta E_f^*$) and Reverse ($\Delta E_r^*$) Elementary Reactions for Methanol Formation on Ni(111) and Pd(111)[a]

| Reaction | $\Delta E_f^*$ | | $\Delta E_r^*$ | |
|---|---|---|---|---|
| | Ni | Pd | Ni | Pd |
| $CO_s + H_s \rightleftarrows HCO_s$ | 23 | 35 | 0 | 0 |
| $HCO_s + H_s \rightleftarrows H_2CO_s$ | 33 | 16 | 26 | 9 |
| $H_2CO_s \rightleftarrows CH_{2,s} + O_s$ | 24 | 34 | 23 | 6 |
| $H_sCO_s + H_s \rightleftarrows CH_3O_s$ | 5 | 10 | 10 | 1 |
| $CH_3O_s \rightleftarrows CH_{3,s} + O_s$ | 13 | 16 | 21 | 12 |
| $CH_3O_s + H_s \rightleftarrows CH_3OH_g$ | 24 | 7 | −5 | 6 |
| $CH_3O_s + H_s \rightleftarrows CH_3OH_s$ | 19 | 7 | 13 | 17 |
| $CH_3OH_g \rightleftarrows CH_{3,s} + OH_s$ | −4 | 10 | 17 | 0 |
| $CH_3OH_s \rightleftarrows CH_{3,s} + OH_s$ | 14 | 22 | 13 | 0 |

[a] See Table 2 for the values of $Q$ and $D + Q$ used in the calculations of $\Delta E^*$. All energies in kcal/mol.

Pd(111) by Guo *et al.* (*16*). It has been shown that there is no isotope mixing, to produce $^{12}C^{16}O$ and $^{13}C^{18}O$, in the desorbing CO, which indicates that the C–O bond rupture does not occur in $CH^3OH_s$ or any of its dehydrogenated products down to $CO_s$. One should add, however, that in XPS and SIMS studies of thermal decomposition of $CH_3OH$ on Pd(111) by Levis *et al.* (*17a,b*), both $CH_3O$–H and $CH_3$–OH bond cleavages have been reported depending on $CH_3OH$ exposure.

In summary, the energetics of CO hydrogenation have been recalculated using a more consistent and accurate form of the BOC-MP approach. The projections presented here have a broader scope and show much better agreement with experiment than those given in our previous work (*1*). Most significantly, we have demonstrated that on Ni the activation barriers for C–O bond dissociation in $H_xCO_s$ ($x = 1$, 3) are smaller than those for the hydrogenation of these species, but that the reverse is true on Pd. Given the thermodynamic preference for formation of $CH_4$ and $H_2O$ over $CH_3OH$, this relationship of the activation barrier heights explains why Ni can produce only $CH_4$, whereas Pd can be selective for both $CH_4$ and $CH_3OH$. Since the heats of adsorption of all species on Pt are very close to those for Pd, the conclusions drawn for Pd should apply as well for Pt.

## ACKNOWLEDGMENTS

Alexis T. Bell acknowledges support of this work by the Division of Chemical Sciences, Office of Basic Energy Sciences, U.S. Department of Energy, under Contract DE-AC03-76SF00098. Both authors thank one of the reviewers for drawing their attention to Ref. (*16*).

## REFERENCES

1. Shustorovich, E., and Bell, A. T., *J. Catal.* **113,** 341 (1988).
2. Shustorovich, E., *Acc. Chem. Res.* **21,** 189 (1988).
3. Shustorovich, E., *in* "Advances in Catalysis" (D. D. Eley, H. Pines, and P. B. Weisz, Eds.), Vol. 37. Academic Press, San Diego, CA, in press.
4. Shustorovich, E., Submitted for publication.
5. Egelhoff, W. H., Jr., *J. Vac. Sci. Technol. A* **5,** 700 (1987).
6. (a) Goodman, D. W., and Campbell, C. T., *Surf. Sci.* **123,** 413 (1982); (b)
7. (a) Whitman, L. J., Richter, L. J., Gurney, B. A., Villarrubia, J. S., and Ho, W., *J. Chem. Phys.* **90,** 2050 (1989); (b) Semanchik, S., and Estrup, P. J., *Surf. Sci.* **104,** 261 (1981); (c) Umbach, E., and Menzel, D., *Surf. Sci.* **135,** 199 (1983).
8. "C. R. C. Handbook of Chemistry and Physics," pp. F171–190. CRC Press, Boca Raton, FL, 1984–1985.
9. Brass, S. G., and Ehrlich, G., *Surf. Sci.* **187,** 21 (1987).
10. (a) Goodman, D. W., *Acc. Chem. Res.* **17,** 194 (1984); (b) Goodman, D. W., Kelly, R. D., Madey, T. E., and White, J. M., *J. Catal.* **64,** 479 (1980).
11. Yates, J. T., Jr., Gates, S. M., and Russell, J. M., Jr., *Surf. Sci.* **164,** L839 (1985).
12. Hall, R. B., Desantolo, A. M., and Bares, S. J., *Surf. Sci.* **161,** L533 (1985).
13. Mori, T., Miyamoto, A., Niizuma, H., Takahashi, N., Hattori, T., and Murakami, Y., *J. Phys. Chem.* **90,** 109 (1986).
14. (a) Rieck, J. S., and Bell, A. T., *J. Catal.* **96,** 88 (1985); (b) Rieck, J. S., and Bell, A. T., *J. Catal.* **99,** 262 (1986).
15. Battacharya, A. K., Chester, M. A., Pemble, M. E., and Sheppard, N., *Surf. Sci.* **206,** L845 (1988).
16. Guo, X., Hanley, L., and Yates, J. T., Jr., *J. Amer. Chem. Soc.* **111,** 3155 (1989).
17. (a) Levis, R. J., Zhicheng, J., and Winograd, N., *J. Amer. Chem. Soc.* **110,** 4431 (1988); (b) Levis, R. J., Zhicheng, J., and Winograd, N., *J. Amer. Chem. Soc.* **111,** 4605 (1989).
18. Santoni, A., Astaldi, C., Della Valle, F., and Rosei, R., *in* "Structure and Reactivity of Surfaces" (C. Mortera, A. Zecchina, and G. Costa, Eds.). Elsevier, Amsterdam, 1989, p. 825.